

Modeling nearshore wave processes*

André J. van der Westhuysen

*UCAR Visiting Scientist at NOAA/NWS/NCEP/EMC Marine Modeling and Analysis Branch
5830 University Research Court, College Park, Maryland 20740, USA
andre.vanderwesthuysen@noaa.gov*

ABSTRACT

This paper provides an overview of recent advances in parameterizing nearshore wave processes within the context of spectral models, and discusses the challenges that remain. Processes discussed include dissipative mechanisms such as depth-induced wave breaking, bottom friction, dissipation due to current gradients, topographical scattering, vegetation, and viscous damping due to fluid mud. Nonlinear processes include near-resonant interaction between triads of wave components, and current-induced nonlinear effects such as amplitude dispersion. Propagation processes include diffraction that takes into account higher-order bathymetry and current gradients. Implementation of these processes in global operational wave modeling systems poses challenges with respect to grid resolution and the availability of model input data. In this regard, a description is given of the Nearshore Wave Prediction System (NWPS), a high-resolution coastal wave modeling system currently under development at NOAA's National Weather Service.

1 Introduction

The first operational third-generation spectral wave models WAM (WAMDIG, 1988) and WAVEWATCH III[®] (Tolman et al., 2002) focused on deep water application, due to a combination of limitations in the description of nearshore physical processes and in computational resources and paradigms. However, as coastal hazards have increased significantly in recent decades (e.g. IPET, 2009), there has been a growing need to extend wave and surge forecast guidance into nearshore areas. This requires detailed, high-resolution modeling that takes into account a number of additional processes to those typically included in deep water basin-scale models, and that has sufficient spatial resolution to properly resolve these processes.

SWAN (Booij et al., 1999) was the first third-generation spectral wave model explicitly designed for nearshore application. In addition to the processes of wind input, nonlinear four-wave interaction, whitecapping and bottom friction dissipation typically accounted for in basin-scale wave models, the nearshore processes of depth-induced breaking and nonlinear three-wave interaction were also incorporated. Since then, a number of advances have been made in the modeling of these nearshore processes and in extending their range of applicability. In addition to these extensions of physics parameterizations, the Courant-Friedrichs-Levy (CFL) stability limitation to the computational time stepping was removed by implementing an implicit numerical scheme. This allowed practical application in coastal regions, using time steps that are appropriate to the time scales of the physical phenomena modeled, as opposed to scales imposed by the numerical framework. Other models, such as WAVEWATCH III and WWM II have followed suit by implementing implicit or quasi-stationary numerical schemes (Roland, 2008; Van der Westhuysen and Tolman, 2011).

However, in addition to revising the physical and numerical frameworks, extending a forecast guidance system to the nearshore also requires alterations to the computational infrastructure. The first step in

* MMAB Contribution No. 298.

this regard was the development of the multi-grid WAVEWATCH III model (Tolman, 2008), which enabled the extension of guidance systems to shelf scales. Subsequently, a number of modeling systems have incorporated high-resolution nearshore nests. Examples of these are the U.S. Navy’s COAMPS-OS system (Cook et al., 2007), and NOAA/National Weather Service’s Nearshore Wave Prediction System (NWPS, Van der Westhuysen et al., 2011), currently in development. These systems, which are connected to the global domain, provide the required resolutions in the nearshore to resolve the small scales of change found there. The development of unstructured grid spectral wave models has provided further possibilities to optimally resolve the vast range of spatial scales found in nearshore regions (Benoit et al., 1996; Hsu et al., 2005; Roland, 2008; Zijlema, 2010).

This paper presents an overview of recent advances in the modeling of nearshore processes, including both the parameterizations of physics and the computational paradigms. It provides an update to previous reviews such as that by The WISE Group (2007). The paper is structured as follows: Section 2 provides an overview of developments in the modeling of the nearshore processes of depth-induced breaking, bottom friction, wave-current interaction and nonlinear three-wave interaction, as well as a number of more localized processes such as coastal reflection, phase-decoupled diffraction, topographic scattering and dissipation due to vegetation. Section 3 discusses the infrastructure required to provide appropriate nearshore resolution by presenting the design features of the NWPS system. Section 4 closes the paper with conclusions.

2 Physical processes

2.1 Action balance equation and source terms

Spectral wind wave models compute the evolution of wave action density N ($= E/\sigma$, where E is the variance density and σ the relative radian frequency) using the action balance equation (e.g. Booij et al., 1999):

$$\frac{\partial N}{\partial t} + \nabla_{x,y} \cdot \left[\left(\vec{c}_g + \vec{U} \right) N \right] + \frac{\partial}{\partial \theta} (c_\theta N) + \frac{\partial}{\partial \sigma} (c_\sigma N) = \frac{S_{\text{tot}}}{\sigma} , \quad (1)$$

with

$$S_{\text{tot}} = S_{\text{in}} + S_{\text{wc}} + S_{\text{nl4}} + S_{\text{bot}} + S_{\text{brk}} + S_{\text{nl3}} \quad (2)$$

The terms on the left-hand side of (1) represent, respectively, the change of wave action in time, the propagation of wave action in geographical space (with \vec{c}_g the intrinsic group velocity vector and \vec{U} the ambient current), depth- and current-induced refraction (with propagation velocity c_θ in directional space θ) and the shifting of the relative radian frequency σ due to variations in mean current and depth (with the propagation velocity c_σ). The right-hand side of (1) represents processes that generate, dissipate or redistribute wave energy, given by (2). In deep water, three source terms are dominant: the transfer of energy from the wind to the waves, S_{in} ; the dissipation of wave energy due to whitecapping, S_{wc} ; and the nonlinear transfer of wave energy due to quadruplet (four-wave) interaction, S_{nl4} . At intermediate depths and in shallow water, the focus of this paper, dissipation due to bottom friction, S_{bot} , depth-induced breaking, S_{brk} , and nonlinear triad (three-wave) interaction, S_{nl3} , are typically accounted for. In addition, parameterizations are available for more localized nearshore processes such as coastal reflection, phase-decoupled diffraction, topographic scattering and dissipation due to vegetation.

The linear kinetic equations, based on geometric optics, that describe the propagation part of (1) are (e.g. Mei, 1983):

$$\frac{d\vec{x}}{dt} = \vec{c}_g + \vec{U} = \frac{1}{2} \left[1 + \frac{2kd}{\sinh 2kd} \right] \frac{\sigma \vec{k}}{k^2} + \vec{U} , \quad (3)$$

$$\frac{d\sigma}{dt} = c_\sigma = \frac{\partial \sigma}{\partial d} \left[\frac{\partial d}{\partial t} + \vec{U} \cdot \nabla d \right] - c_g \vec{k} \cdot \frac{\partial \vec{U}}{\partial s} , \quad (4)$$

$$\frac{d\theta}{dt} = c_\theta = -\frac{1}{k} \left[\frac{\partial \sigma}{\partial d} \frac{\partial d}{\partial m} + \vec{k} \cdot \frac{\partial \vec{U}}{\partial m} \right] , \quad (5)$$

where s is the space coordinate orthogonal to the wave crest, m the coordinate along the wave crest, k the wavenumber and d the depth.

2.2 Depth-induced breaking

As the primary dissipation mechanism in the surf zone, depth-induced breaking is a crucial component of wave models that resolve the nearshore. Two basic approaches have been proposed to describe this process, namely the roller model (Duncan, 1981, 1983) and the bore model (e.g., Stoker, 1957, Battjes and Janssen, 1978). The most widely-used phase-averaged description is the bore-based model of Battjes and Janssen (1978):

$$D_{tot} = -\frac{1}{4} \alpha_{BJ} Q_b \left(\frac{\bar{\sigma}}{2\pi} \right) H_m^2 , \quad (6)$$

with

$$\frac{1 - Q_b}{\ln Q_b} = -8 \frac{E_{tot}}{H_m^2} , \quad (7)$$

where α_{BJ} is a proportionality coefficient, $\bar{\sigma}$ is the mean radian frequency, E_{tot} the total variance and $\gamma = H_m/d$ the breaker index, based on the shallow water limit of the breaking criterion of Miche (1944). At each local depth d , the breaker index γ determines the maximum wave height H_m of unbroken waves. From this, the fraction of breakers Q_b in the wave field is implicitly solved in (7). This, in turn, is used in (6) to solve for the bulk breaking-induced dissipation over the wave spectrum. Thornton and Guza (1983) modified this expression to better take into account the distribution of breaking wave heights. The source term can be compiled from (6) by assuming that the dissipation per spectral component is proportional to its variance density (Battjes and Beji, 1992; Booij et al., 1999):

$$S_{brk}(\sigma, \theta) = D_{tot} \frac{E(\sigma, \theta)}{E_{tot}} \quad (8)$$

However, Herbers et al. (2000) have shown that depth-induced breaking forms a close balance with three-wave interactions in the surf zone. In this regard, Chen et al. (1997) propose a frequency squared distribution of the breaking dissipation over the spectrum.

The bore-based model of Battjes and Janssen (1978) has been shown to perform well over a wide variety of beach conditions. The value of the breaker index γ has been parameterized by a number of researchers (e.g. Battjes and Stive, 1985; Nelson, 1994; Ruessink et al., 2003; Apotsos et al., 2008). However, the performance is less positive in enclosed, shallow areas, such as inter-tidal regions and shallow lakes. To address this issue, Van der Westhuysen (2010) analyzed optimal values of γ under a wide range of

field and laboratory conditions. It was found that the optimal value of γ , based on minimizing the bias and scatter index, can be divided into two populations: one for sloping beaches (waves generated in deep water, subsequently breaking on a beach) and one for finite-depth wave growth cases (local wave growth over shallow, enclosed areas). For both wave height and wave period, the sloping beach cases show a minimum error for γ values around 0.6–0.8, i.e. around the commonly-used default of $\gamma = 0.73$. By contrast, for cases with finite depth growth over nearly-horizontal beds, the errors are monotonically decreasing with increasing γ , with optimal values at $\gamma > 0.9$. Thus, in the equilibrium balance, depth-limited breaking has a smaller dissipation contribution in the case of finite-depth wave growth than in the case of sloping beaches. Here the input by the wind is balanced by the dissipation through whitecapping and bottom friction. Previous parameterizations for γ , typically developed for sloped beaches, did not adequately describe this dynamic behaviour.

Van der Westhuysen (2010) proposes to modify the breaker formulation by Thornton and Guza (1983) to provide accurate results in finite-depth wave growth conditions whilst retaining good performance over sloping beaches. Van der Westhuysen (2010) shows that the fraction of breaking waves in this model can be expressed as a power law of the biphasic (β) of the self-interactions of the spectral peak, which, along with the skewness and asymmetry, is a measure of the shallow water nonlinearity of the waves. As waves propagate from deeper water (where they are approximately sinusoidal) to intermediate depth, they become more “peaked” or skewed, but symmetrical ($\beta = 0$), and in shallow water they have a saw tooth shape and they become asymmetric ($\beta \rightarrow -\pi/2$) and break. Since waves that are generated locally in finite depth have lower levels of nonlinearity at the same depth than waves generated offshore in deep water, the breaking dissipation is less. Because SWAN is not a nonlinear phase-resolving model, it cannot compute the biphasic of the waves. However, Doering and Bowen (1995) and Eldeberky (1996) related the biphasic to the Ursell number, which can be computed by SWAN, so that the problem can be closed. The resulting biphasic breaker model is given by Van der Westhuysen (2009, 2010):

$$D_{\text{tot}} = -\frac{3\sqrt{\pi} B^3 \tilde{f}}{16 d} \left(\frac{\beta}{\beta_{\text{ref}}} \right)^n H_{\text{rms}}^3, \quad (9)$$

in which B is a proportionality coefficient, \tilde{f} the mean frequency and β_{ref} the reference biphasic at which all waves are breaking. The exponent n relates the biphasic to the fraction of breaking waves, which is dependent on the mean wave steepness (Van der Westhuysen, 2009). The reference biphasic is set at $\beta_{\text{ref}} = -4\pi/9 = -1.396$ based on laboratory data of Boers (1996). The value of the parameter $B = 0.98$ was determined by means of calibration to a wide range of field and laboratory observations.

Salmon and Holthuijsen (2011) propose a new parameterization of the breaker index γ which takes into account dispersion $\tilde{k}d$ (after Ruessink et al., 2003 and Van der Westhuysen, 2010) and a mean bed slope. From a data set based on that of Van der Westhuysen (2010), with additional sloped beach and reef profile laboratory cases, they derive the following parameterization: $\gamma = 1$ at high $\tilde{k}d$ (large and intermediate dimensionless depths) reducing to $\gamma = 0.5$ – 0.6 at $\tilde{k}d \approx 0.5$ (small dimensionless depth). At these low values of $\tilde{k}d$, the value of the breaker index is found to only depend on the mean bed slope, decreasing monotonically with the latter within this $\gamma = 0.5$ – 0.6 range. Note that this bed slope parameterization has little bearing on inter-tidal seas and shallow lakes with near-horizontal beds, since their relatively high $\tilde{k}d$ values places them outside of this range (e.g. Young and Babanin, 2006; Van der Westhuysen, 2010, Figure 9). Also, in some cases, reef profiles are not characterized by their (very steep) leading slopes, where the breaking initialization and most of the dissipation occur, but rather the near-horizontal slopes of the reef tops.

Filipot et al. (2010) and Filipot and Ardhuin (2012) propose a parameterization that unifies the breaking processes that have traditionally been divided into deep water “whitecapping” and finite-depth “depth-induced breaking” regimes. They argue that, whatever the water depth, waves break when their crest orbital velocity u_c approaches their phase velocity c . Based on this principle, a breaking criterion $u_c/c \approx$

1 is defined, which can be expressed, for regular waves, as $kH/\tanh(kh) \approx \beta_t$, with $\beta_t = 0.88$ a breaking threshold (Miche, 1944). From this, a single wave breaking source term is composed, which is shown to be valid from the deep ocean to the surf zone.

The energy lost by waves is first explicitly calculated in physical space and subsequently distributed over the relevant spectral components. Each wave scale is centered on a frequency f_i with a finite bandwidth $f_{i,-} = 0.7f_i$ to $f_{i,+} = 1.3f_i$, from which a representative wave height and wavenumber are computed. From these, parameterizations of the breaking probability $Q(f_i)$ (using a linearized version of β_t), a crest length density $\Pi(f_i)$ and a dissipation rate per unit length of breaking crest $\varepsilon(f_i)$ are defined for each scale. The dissipation rate $\varepsilon(f_i)$ is a key component in this parameterization, and is composed from Duncan (1981) and a modified version of Chawla and Kirby (2002). For details see Filipot and Ardhuin (2012). The product of $Q(f_i)$, $\varepsilon(f_i)$ and $\Pi(f_i)$ yields a dissipation rate per unit area, $D(f_i)$, for each scale f_i . This enables a seamless transition from deep to shallow water. The dissipation rate $D(f_i)$ is subsequently attributed to the spectral components that contribute to the scale f_i :

$$S_{\text{bk},i}(f) = \frac{D(f_i) \times E(f)}{\int_0^\infty E(f) W_i(f) df} , \quad (10)$$

where $W_i(f)$ is a filtering window that is equal to unity over the frequencies $f_{i,-}$ to $f_{i,+}$ and zero elsewhere. The source term for each frequency f is associated with several wave scales, from f_j to f_k , so that the final source term reads:

$$S_{\text{bk}}(f) = \frac{1}{k-j+1} \sum_{i=j}^k S_{\text{bk},i}(f) \quad (11)$$

Model results using this expression are shown to yield comparable accuracy to those obtained using the specialized deep and shallow water parameterizations of Bidlot et al. (2005), Ardhuin et al. (2010) and Battjes and Janssen (1978) with $\gamma = 0.73$.

2.3 Bottom friction

Energy loss due to the interaction of the wave orbital motion with the sea bed is typically described using the following hydrodynamic friction model:

$$S_{\text{bot}}(\sigma, \theta) = -C_{\text{bottom}} \frac{\sigma^2}{g^2 \sinh^2(kd)} E(\sigma, \theta) \quad (12)$$

Three descriptions of the proportionality coefficient C_{bottom} have emerged. The first, proposed by Hasselmann et al. (1973), is to assume C_{bottom} to be an empirically-derived constant. A value of $0.038 \text{ m}^2/\text{s}^3$ was proposed by these authors. Bouws and Komen (1983) showed a value of $0.067 \text{ m}^2/\text{s}^3$ to be more appropriate for wind seas observed during the TMA experiment, compared to the former value which is more appropriate for swell. Zijlema et al. (2012) propose a value of $0.038 \text{ m}^2/\text{s}^3$ for both swell and wind sea, based on a reanalysis of the TMA data. The latter setting is confirmed by Van der Westhuysen et al. (2012) on the basis of observations and hindcasting in the Dutch Wadden Sea.

The second approach, proposed by Hasselmann and Collins (1968) and Collins (1972), is to apply a drag law model to C_{bottom} :

$$C_{\text{bottom}} = f_w g U_{\text{rms}} , \quad (13)$$

in which the friction factor f_w is taken as a universal constant. However, the use of a constant friction factor is physically incorrect, since it is not f_w , but rather the bed roughness that, for a given seabed state, is constant (Tolman, 1994). Hence, this model is generally not recommended for application. The third approach is the eddy viscosity model of Madsen et al. (1988):

$$C_{\text{bottom}} = f_w g U_{\text{rms}} / \sqrt{2} , \quad (14)$$

in which the friction factor f_w is not constant, but a function of the Nikuradse roughness k_N , given by the expressions of Jonsson (1966), Jonsson and Carlsen (1976) and Jonsson (1980). In turn, this hydrodynamic roughness k_N can vary over a number of orders of magnitude from sand grain roughness to ripple roughness (Shemdin et al., 1978). A number of movable bed models have been proposed to describe the evolution of the hydrodynamic roughness from sand grain roughness (or relic bed forms), through ripple formation, to ultimately the washing out of all structures under severe wave conditions. Grant and Madsen (1982) present a ripple model for monochromatic waves, which can be applied to random waves by using an equivalent monochromatic wave (Mirfenderesk, 1999; Mirfenderesk and Young, 2003). Nielsen (1992), by contrast, derived a ripple model specifically for random waves. All these expressions are based on non-cohesive sediments, and require information on the D_{50} sand grain distribution and relic bed forms (initial conditions).

Eddy viscosity bed friction models, combined with movable bed roughness models, are considered the state of the art in accounting for hydrodynamic bed friction losses. Graber and Madsen (1988) implemented the hydraulic bottom friction model of Madsen et al. (1988) in a parametric wind wave model together with the Grant and Madsen (1982) ripple model, using a representative monochromatic wave. Tolman (1994) applied the friction model of Madsen et al. (1988) in the third-generation model WAVEWATCH, together with a modified version of Grant and Madsen (1982) to correct shortcomings of this model regarding irregular waves. Ardhuin et al. (2003a,b) applied a modified version of the Tolman (1994) model, re-calibrated to field conditions found during the SHOWEX experiment. Smith et al. (2011) recently implemented and verified the model of Nielsen (1992) in the nearshore model SWAN.

A challenge in applying movable bed roughness models is the general unavailability of information on sand grain distributions and relic bed forms and, failing that, the difficulty of providing a generalized D_{50} value for universal application. In addition, initial ripple formation results in a strong discontinuity in the friction factor f_w (e.g. Tolman, 1994), which occurs at spatial decay scales that are typically not resolved by large-scale wave models. Therefore, Tolman (1995) proposes a subgrid moveable-bed bottom friction model that defines a representative bottom roughness in the large-scale model, based on the local application of a discontinuous roughness model such as those discussed above, with a statistical description of depth, sediment and wave parameters.

2.4 Wave-current interaction

Currents have an influence on both the wave kinematics and dynamics. As waves propagate into a region with a negative current gradient (e.g. opposing current increasing in strength) waves are Doppler shifted and become shorter and steeper; conversely, as they propagate into a positive gradient (e.g. following current increasing in strength) waves become elongated and less steep; when current gradients are met obliquely, current-induced refraction occurs (e.g. Phillips, 1977; Holthuijsen and Tolman, 1991; Haus, 2007; Zhang et al., 2009). Barber (1949) and Tolman (1991) discuss the implications of nonstationarity on these interactions. These phenomena are described by the linear kinematic equations (3–5), and the conservation of wave action in ambient current is represented in the action balance equation (1). Dynamic effects include the influence of the current on the wave growth, the so-called wave age effect: waves entering an opposing current have an effectively lower wave age, resulting in stronger momentum transfer from the wind, and vice versa for following currents (Haus, 2007; Van der Westhuysen et al.,

2012). This too is included in the action balance equation (1). However, preliminary results suggest that the situation is more complex when considering the atmosphere, waves and current field as a coupled system: since the current field influences the atmospheric boundary layer, some of the aforementioned effects are canceled out (Hersbach and Bidlot, 2008).

When waves approach a strong negative current gradient, such as found in tidal inlets, they steepen and break. When the opposing current velocity matches the wave group velocity, waves become blocked (e.g. Shyu and Phillips, 1990; Lai et al., 1989; Chawla and Kirby, 2002; Suastika, 2004). Under partial blocking conditions, Ris and Holthuijsen (1996) show that wave energy can be significantly overestimated by spectral models such as SWAN. Using laboratory cases, studies by Ris and Holthuijsen (1996), Chawla and Kirby (2002) and Suastika (2004) show that such overestimation can be addressed by applying enhanced levels of whitecapping dissipation based on wave steepness. This is in addition to the lower levels of whitecapping dissipation typically calibrated to balance wind input S_{in} . However, Van der Westhuysen (2012) shows that wave steepness is not an effective predictor in complex field situations, since this results in the excessive dissipation of young, inherently steep wind sea. Instead, it is proposed to scale the enhanced level of whitecapping dissipation with the normalized degree of Doppler shifting per spectral bin, given by c_{σ}/σ , thereby isolating the steepening effect of the current:

$$S_{wc,cur}(\sigma, \theta) = -C''_{ds} \max \left[\frac{c_{\sigma}(\sigma, \theta)}{\sigma}, 0 \right] \left[\frac{B(k)}{B_r} \right]^{\frac{p}{2}} E(\sigma, \theta) , \quad (15)$$

in which the propagation in σ space c_{σ} is given by (4). Here $B(k)$ is the saturation spectrum with a threshold saturation level B_r and p is a wave-age dependent exponent, which are defined and calibrated in Van der Westhuysen et al. (2007). The calibration coefficient C''_{ds} was found based on laboratory data, where the process of wave-induced steepening could be isolated. A maximum function is included in (15) in order to take only relative increases in steepness into account in the enhanced dissipation. Note that negative current gradients occur both for accelerating opposing currents and decelerating following currents, both of which result in steepening of the waves. Experimental evidence of the latter phenomenon was found by Babanin et al. (2011).

As waves approach the blocking point, they become increasingly nonlinear, making the linear action balance equation (1), the linear kinematic expressions (3)–(5) and the above-mentioned dissipation approaches inadequate. A nonlinear extension to (1) has been proposed by Willebrand (1975), who describes a number of impacts: (i) the group velocity magnitude and direction are altered (amplitude dispersion), (ii) the refraction term may be non-vanishing even if the mean current and depth are horizontally homogeneous and (iii) a higher-order correction to the radiation stress effects.

Diffraction due to gradients in the bathymetry or current field is another important extension to the geometric optics-based expressions (1)–(5). Since no phase information is retained in (1), Holthuijsen et al. (2003) propose a phase-decoupled approach for incorporating diffraction into (1). This is derived from the Berkhoff (1972) time-harmonic mild slope equation (MSE), in the absence of currents. Hsu et al. (2006) points out that this approach is inconsistent with the action balance equation (1), since the diffraction corrections were not derived for waves in the presence of currents. They present an improved phase-decoupled expression, derived from the time-harmonic extended MSE that includes the influence of currents. They show improved results in the vicinity of strong current gradients, such as over rip currents. Toledo et al. (2012) continue this effort by deriving an extended, time-dependent MSE that retains higher-order terms for changes in bottom profiles and ambient currents, from which an extended action balance equation is produced.

The models discussed above, including the action balance equation (1), all regard depth-averaged currents. The vertical structure of the current can, however, have a significant effect on the results. The generalized Lagrangian mean theory of Andrews and McIntyre (1978) provides exact equations for the description of interaction between waves, turbulence and the mean flow in three dimensions. For practi-

cal application, these must be closed by specifying the wave forcing terms, which can ultimately be expressed in terms of the wave spectrum. Expressions for this system of equations have been proposed in a series of papers by Mellor (2003, 2005), Ardhuin et al. (2008a,b), Mellor (2011a,b), Bennis and Ardhuin (2011) and Aiki and Greatbatch (2012a,b).

2.5 Nonlinear three-wave interaction

As dispersion decreases in water of finite depth, interactions between groups of three waves, or triads, become near-resonant, approximately satisfying the conditions:

$$f_1 \pm f_2 = f_3 \quad (16)$$

and

$$\vec{k}_1 \pm \vec{k}_2 = \vec{k}_3 \quad (17)$$

These interactions represent a second-order Stokes-type nonlinearity, which, when near-resonant (typically in the surf zone), results in a strong exchange of wave energy, transforming the spectrum within a few wave lengths. These result in sub- and superharmonics of the spectral peak, which are associated with phenomena such as nonlinear wave profiles (sharp crests and flat troughs, transitioning to saw-tooth shaped crests at incipient breaking) and surf beat. These interactions are contrasted with the weaker, third-order interactions between a quadruplet of waves, which are resonant in deep water, and require thousands of wavelengths to have a significant effect (e.g. Hasselmann, 1962). Stochastic expressions for three-wave interaction are found by ensemble averaging deterministic evolution equations. Given the one-dimensional transport equation for the Fourier components ζ_p of a random wave field:

$$\frac{d}{dx} \zeta_p = ik_p \zeta_p + i \sum_{n+m=p} W_{nm} \zeta_n \zeta_m, \quad (18)$$

ensemble averaging results in a hierarchy of increasingly higher-order evolution equations, given symbolically as (e.g. Janssen, 2006):

$$d_x \langle \zeta \zeta \rangle = \langle \zeta \zeta \rangle + \langle \zeta \zeta \zeta \rangle^C \quad (19)$$

$$d_x \langle \zeta \zeta \zeta \rangle = \langle \zeta \zeta \zeta \rangle + \langle \zeta \zeta \rangle \langle \zeta \zeta \rangle + \langle \zeta \zeta \zeta \zeta \rangle^C \quad (20)$$

$$d_x \langle \zeta \zeta \zeta \zeta \rangle = \langle \zeta \zeta \zeta \zeta \rangle + \langle \zeta \zeta \rangle \langle \zeta \zeta \zeta \rangle + \langle \zeta \zeta \zeta \zeta \zeta \rangle^C \quad (21)$$

$$\vdots$$

Equation (19) describes the evolution of the variance density spectrum, with d_x the spatial derivative and $\langle \dots \rangle$ an ensemble average. The term $\langle \zeta \zeta \zeta \rangle^C$ is the third cumulant, which is the residue after decomposing the moment in products of lower order. This cumulant represents the process of nonlinear three-wave interaction. Solving this term requires information from the higher-order bispectral evolution equation (20). The latter, in turn, contains a fourth cumulant, $\langle \zeta \zeta \zeta \zeta \rangle^C$, which must be computed by means of the trispectral evolution equation (21), and so on. It is therefore necessary to implement a closure approximation. One option is to apply a closure to the fourth cumulant, leaving a coupled system of spectral and bispectral equations.

Various approaches have been proposed regarding the choice of underlying deterministic equations and the closures applied. Earlier studies have applied the Zakharov kinetic integral (e.g. [Eldeberky, 1996](#)) and Boussinesq equations (e.g. [Herbers and Burton, 1997](#); [Kofoed-Hanssen and Rasmussen, 1998](#)) which have dispersion limits, whereas full-dispersion equations were applied in more recent work (e.g. [Agnon and Sheremet, 1997](#); [Eldeberky and Madsen, 1999](#); [Janssen et al., 2008](#)). Closure approximations include the so-called quasi-normal closure, in which the fourth cumulant is set to zero ([Benney and Saffman, 1966](#)), an approach where the fourth cumulant is assumed proportional to the third moment ([Holloway, 1980](#)), and an approach in which the cumulant is relaxed to a Gaussian state ([Herbers et al., 2003](#); [Janssen, 2006](#)). The latter approach avoids physically unrealistic oscillations in shallow water found with the quasi-normal closure. A major remaining challenge is finding a two-dimensional evolution equation for the bispectrum, since it is comprised of three distinct spectral components, each propagating along their own wave ray. Without this, a fully isotropic description of three-wave interactions is not possible. The present state of the art is a model for two-dimensional nonlinear interaction, over topography with mild changes in the lateral direction ([Janssen et al., 2008](#)).

The two-equation system (spectrum and bispectrum) is, however, computationally expensive, and not suitable for operational wave modeling. As a result, approximations have been proposed to reduce the computational time. [Eldeberky \(1996\)](#) and [Becq-Girard et al. \(1999\)](#) propose to spatially integrate the bispectral evolution equation, thereby achieving a single transport equation for the energy spectrum. Note that these expressions are for the one-dimensional case. Since the spatial evolution of the bispectrum and phase coupling are not computed, they do not reproduce the release of harmonics in increasing depth (e.g. behind a bar). The question of spatial propagation is solved by assuming that all interactions are collinear, and applying the one-dimensional interaction expression in each spectral direction. This results in an isotropic description suitable for practical model application. [Eldeberky \(1996\)](#) makes the further simplification to include only self sum interactions, producing only the first ($2f_p$), third ($4f_p$), etc., superharmonics, and no subharmonics. All variables, including the interaction coefficient and the phase of the bispectrum, are parameterized as local quantities. The resulting model, the Lumped Triad Interaction (LTA) is fast, but has only been found to perform sufficiently over simple beach profiles and the seaward face of bars ([Becq-Girard et al., 1999](#)).

[Stiassnie and Drimer \(2006\)](#) and [Toledo and Agnon \(2012\)](#) propose an approach that is midway between the two-equation expression of [Janssen et al. \(2008\)](#) and others and the approximate LTA of [Eldeberky \(1996\)](#) in terms of speed and accuracy. They base their work on [Agnon and Sheremet \(1997, 2000\)](#), who produced one-equation models containing all interactions, which feature both local and non-local (i.e. containing spatial integrals) shoaling coefficients. [Stiassnie and Drimer \(2006\)](#) and [Toledo and Agnon \(2012\)](#) localize these coefficients by omitting contributions that transfer energy back and forth between harmonics (retaining only the mean energy transfer) as well as higher-order bottom interaction terms. Fewer assumptions are made than in the derivations of [Eldeberky \(1996\)](#) and [Becq-Girard et al. \(1999\)](#). The expression of [Toledo and Agnon \(2012\)](#) shows good results in reproducing the first ($2f_p$) and second ($3f_p$) superharmonics. This expression describes one-dimensional interaction, which can be included in an isotropic description in spectral wave models.

2.6 Other processes

A number of additional processes that are of importance in specific nearshore situations have been described in the literature. These include extensions to the geometrical optics-based kinematic equations presented in Section 2.1, such as coastal reflection and topographic scattering, and also wave field evolution due to interaction with vegetation and fluid mud.

Descriptions of coastal reflection have been included in phase-averaged wave models by [Benoit et al. \(1996\)](#), [Booij et al. \(2004\)](#) and [Ardhuin and Roland \(2012\)](#). See also [Ilic et al. \(2007\)](#). Since phase information is not retained in (1), a complete phase-coherent description of incoming and reflected wave

trains is not possible. Instead, the directional variance density spectrum is mirrored about the axis of the coastline, taking into account a reflection coefficient and a degree of scattering. The amount of reflection is dependent on the shoreface slope, the mean frequency and incident wave height. Integration over the directional spectrum then yields the total variance of both the incoming and reflected components. As such, these phase-averaged approaches are not considered suitable in regions where phase-coherent structures are expected (e.g. standing waves inside harbor basins and close to sea walls). They do, however, provide meaningful results in the far field, where wave components are more scattered. [Ardhuin and Roland \(2012\)](#) find reflection to be significant at field sites in the coastal waters along the U.S. West Coast and the Hawaiian Islands, and necessary to reproduce buoy observations there. The most significant impact is to the directional spreading of the wave field, which is greatly increased by the reflected components.

Waves can interact with the seabed at various scales, as discussed by [Ardhuin et al. \(2003a\)](#). Interaction with large-scale bathymetric features (> 1 km) result in refraction and shoaling, which are described by (1), (3) and (5). At smaller scales, waves are scattered by the bottom through the process of Bragg scattering, descriptions of which are given by [Hasselmann \(1966\)](#), [Long \(1973\)](#) and [Ardhuin and Herbers \(2002\)](#). Bathymetrical features at the scale of a few wavelengths scatter waves forward, resulting in the broadening of the directional spectrum ([Ardhuin and Herbers, 2002](#)). Features at scales shorter than a wavelength cause backscattering, which results in dissipation of wave energy ([Long, 1973](#)). As such, the ability to incorporate Bragg scattering depends on the scales at which the coastal bathymetrical data is available and resolved in the wave model. In operational systems, the bathymetry is typically not resolved at scales of less than a wavelength (see below), so that only refraction, and potentially forward scattering, can be incorporated at present.

Wave energy is dissipated by aquatic halophytic vegetation such as salt marshes and mangroves that occur in the inter-tidal zone in tropical and temperate coasts. A frequently applied approach to account for energy losses due to vegetation is through the bottom friction parameterization. [Quartel et al. \(2007\)](#) found from field observation that wave attenuation due to the equivalent bed roughness of mangrove vegetation is four times higher than that due to a sandy bed. This approach is, however, highly empirical. A more fundamental approach is to account for these dissipation losses in terms of the work done by the vegetation through the plant-induced drag forces on the water column, expressed in terms of a [Morrison et al. \(1950\)](#) type expression ([Dalrymple et al., 1984](#); [Kobayashi et al., 1993](#); [Vo-Luong and Massel, 2008](#)). [Dalrymple et al. \(1984\)](#) proposed a formulation for wave damping that considers a field of cylinders extending to some fraction of the water column, for normally incident waves in water of an arbitrary, but constant depth. [Mendez and Losada \(2004\)](#) extended this expression by accounting for variable water depth, and narrow-banded random uni-directional waves, including wave breaking. The bulk drag coefficient for a given vegetation type is parameterized with respect to the Keulegan-Carpenter number, taking into account the vegetation diameter, density and height. [Suzuki et al. \(2011\)](#) extended the [Mendez and Losada \(2004\)](#) formulation by including a vertical layer schematization, enabling the description of layered vegetation such as mangroves. An isotropic description for use in spectral wave models is obtained by applying the bulk vegetation-induced dissipation proportional to the directional variance density spectrum.

Fluid mud deposits in coastal regions affect waves through viscous damping, alteration of the dispersion relation and through the associated change in group velocity. As such, fluid mud affect the wave climate, and can afford coastal protection during storm events. The extended dispersion relation and energy-dissipation equation are typically obtained from a viscous two-layer model schematization. [Kranenburg et al. \(2011\)](#) discuss the most commonly used descriptions, namely those of [Gade \(1958\)](#), [Dalrymple and Liu \(1978\)](#), [De Wit \(1995\)](#) and [Ng \(2000\)](#). The model of [Gade \(1958\)](#) has been derived for shallow water conditions, the model of [Ng \(2000\)](#) for mud layers with a thickness of less than or equal to the Stokes boundary layer thickness, and that of [Dalrymple and Liu \(1978\)](#) for deeper water and thicker fluid mud layers. The more general model of [De Wit \(1995\)](#) covers the full range of

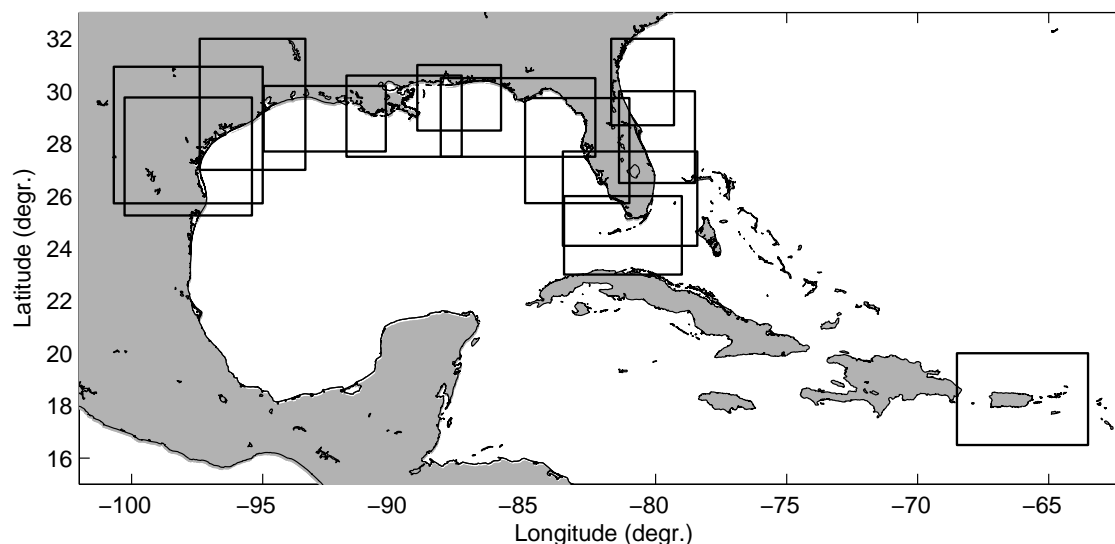


Figure 1: NWPS nearshore wave model nests for the National Weather Service's Southern Region, containing the southern states of the USA and Puerto Rico.

conditions expected to occur in coastal areas. [Rogers and Holland \(2009\)](#) implemented the dispersion relation of [Ng \(2000\)](#) and the viscous dissipation expression of [Soltanpour et al. \(2003\)](#) into the wave model SWAN. [Kranenburg et al. \(2011\)](#) derived a dispersion relation and dissipation equation based on the approach of [De Wit \(1995\)](#), also implementing it in SWAN. The latter implementation is considered more generic than that of [Rogers and Holland \(2009\)](#) since it covers the full range of expected coastal conditions. A challenge in the operational application of these expressions is the poor availability of input data, including the spatial extent of the mud deposit, its thickness, density and viscosity. In addition to the viscous effects discussed here, the effects of elasticity, porosity and plasticity in the mud layer can also be included in the description (e.g. [MacPherson, 1980](#); [Maa, 1986](#); [Mei and Liu, 1987](#); [Liu, 1973](#); [Verbeek and Cornelisse, 1997](#)).

3 Multi-scale modeling

In order to adequately model the nearshore processes discussed in the sections above, the spatial scales over which they occur need to be properly resolved. The global multi-grid version of WW3 ([Tolman, 2008](#)), run operationally at the National Centers for Environmental Prediction (NCEP), covers the globe at a 1/2 degree resolution, with two-way nesting down to 4 arc-min over shelf regions. The latter resolution is, however, still insufficient for resolving nearshore details such as tidal inlets, barrier islands, coastal currents and surf zones, and hence many of the processes discussed above.

The National Weather Service is addressing this modeling need by developing the Nearshore Wave Prediction System (NWPS; [Van der Westhuysen et al., 2011](#)), which will comprise a series of high-resolution coastal nests covering all U.S. coastal waters, including the Great Lakes. Figure 1 shows the NWPS domains in the southern United States, including Puerto Rico. Each of the nests is run locally at a coastal Weather Forecast Office (WFO), receiving its boundary conditions from the centrally run global multi-grid WAVEWATCH III model. These coastal domains typically have a resolution of 1 nmi, reduced down to 10 m in focus areas (e.g. tidal inlets) by further nesting. In addition to wave inputs, the nearshore domains ingest current fields from the HYCOM-based Real-Time Ocean Forecast System (RTOFS, [Mehra and Rivin, 2010](#)), and water levels, including tides and surge, from the ADCIRC-based Extra-tropical Surge and Tide Operational Forecast System (ESTOFS), currently in

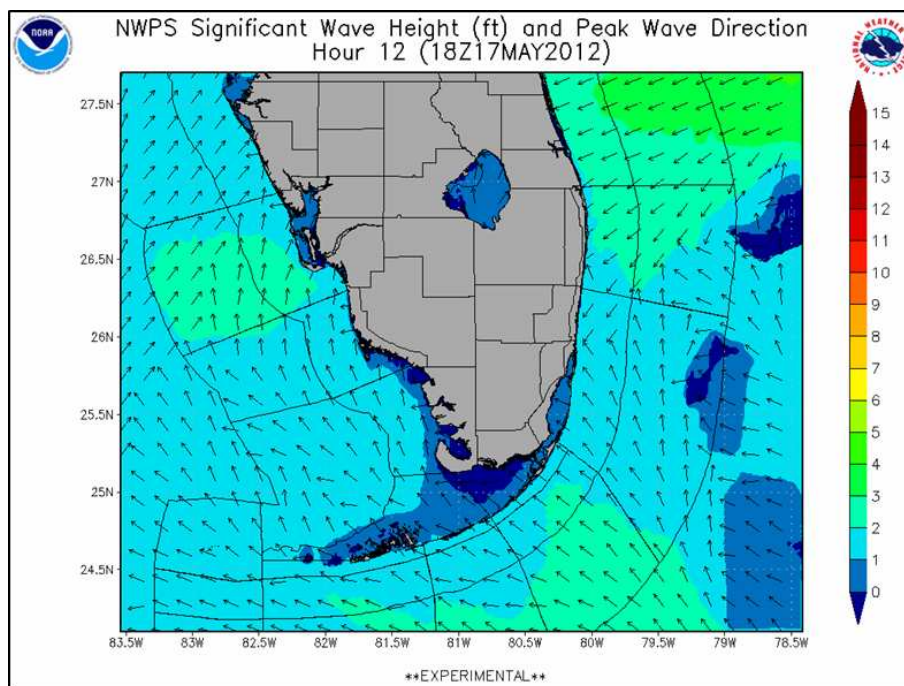


Figure 2: Example of NWPS significant wave height output for the WFO Miami domain on its coarsest model grid of 1 nmi resolution (Source: NOAA, www.srh.noaa.gov/mfl/?n=NWPS).

development. Figure 2 shows example output of NWPS over the WFO Miami domain. The influence of the Gulf Stream on the wave field in this domain is demonstrated by [Settelmaier et al. \(2011\)](#). The NWPS system is being integrated into the Advanced Weather Interactive Processing System (AWIPS) II which manages all data flows and data display at WFOs. In future, NWPS will be extended to run on unstructured grids, to be able to optimally resolve the widely varying spatial scales found in nearshore regions (Figure 3). In addition, the system will incorporate a local, two-way coupled wave-surge model to also capture the influence of the waves on surge levels, based on the work of [Dietrich et al. \(2011\)](#).

4 Conclusions

This paper presented an overview of nearshore processes that are relevant to operational wave modeling, and discussed recent parameterizations for phase-averaged models. In addition, the infrastructural aspects of providing adequate nearshore resolution to resolve these processes were discussed. Dissipative nearshore process considered include depth-induced breaking, bottom friction, current gradients, topographical scattering, vegetation and viscous damping due to fluid mud. Nonlinear and propagation processes considered include near-resonant interaction between triads of wave components, and current-induced nonlinear effects such as amplitude dispersion and diffraction.

With a few exceptions, the primary obstacles to including these processes are the availability of adequate input data and providing sufficient model resolution to resolve the relevant processes. In particular, advanced formulations for bottom friction require knowledge of the D_{50} grain size distribution, damping by fluid mud requires knowledge of the spatial extent, thickness, density and viscosity of the mud deposit, and dissipation by vegetation requires information on the thickness, length, vertical structure and density of each vegetation type included. As such, these processes may be challenging, but not impossible, to include in regional operational models extending to the nearshore. By contrast, with sufficient nearshore resolution (scale of 20–100 m) nearshore processes such as bottom friction, depth-included

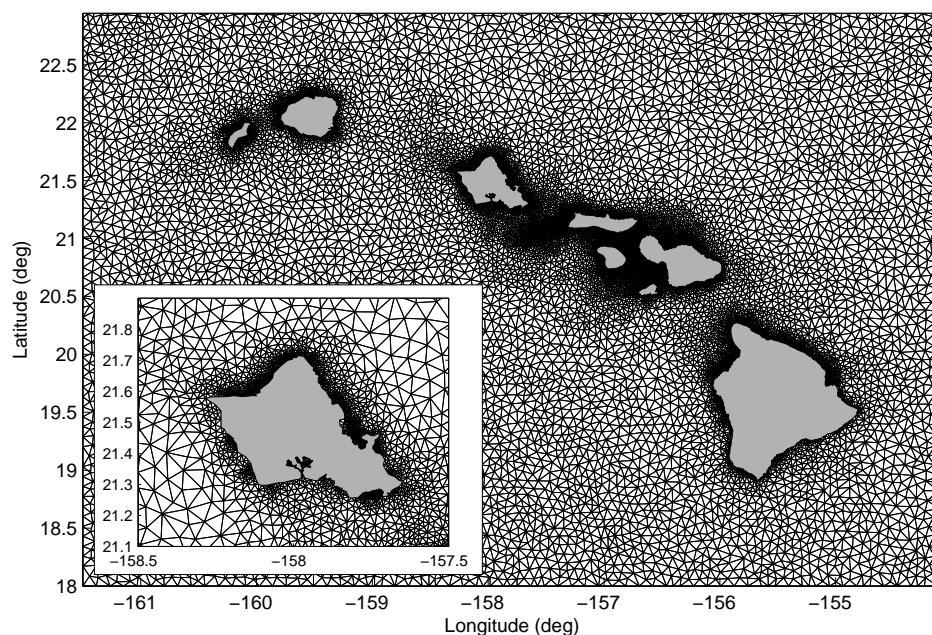


Figure 3: Example of an unstructured computational grid for WFO Honolulu, USA, covering all of the Hawaiian Islands. Inset shows detail for the island of Oahu. Note the strong variation in grid resolution from deep to nearshore water.

breaking and triad interaction can be included effectively. It was discussed how the National Weather Service provides the required high-resolution grids and model input through the Nearshore Wave Prediction System (NWPS). Some nearshore processes, however, remain beyond practical application at present, due to their high demands on spatial and/or temporal resolution. These include Bragg backscattering, and two-equation representations of nonlinear triad interactions describing the evolution of the bispectrum.

Acknowledgements

I thank Hendrik Tolman and Yaron Toledo for their valuable comments on this manuscript.

References

- Agnon, Y. and A. Sheremet, 1997: Stochastic nonlinear shoaling of directional spectra. *J. Fluid Mech.*, **345**, 79–99.
- Agnon, Y. and A. Sheremet, 2000: *Stochastic evolution models for nonlinear gravity waves over uneven topography*. Advances in Coastal and Ocean Engineering: Volume 6, Edited by: Philip L-F Liu. World Scientific.
- Aiki, H. and R. Greatbatch, 2012a: Thickness-weighted mean theory for the effect of surface gravity waves in mean flows in the upper ocean. *J. Phys. Oceanogr.*, **42**, 725–747.
- Aiki, H. and R. Greatbatch, 2012b: The vertical structure of the surface wave radiation stress for circulation over a sloping bottom as given by thickness-weighted-mean theory. *J. Phys. Oceanogr.*, doi:10.1175/JPO-D-12-059.1, in press.

- Andrews, D. G. and M. E. McIntyre, 1978: An exact theory of nonlinear waves on a Lagrangian-mean flow. *J. Fluid Mech.*, **89**, 609–646.
- Aptosos, A., B. Raubenheimer, S. Elgar and R. T. Guza, 2008: Testing and calibrating parametric wave transformation models on natural beaches. *Coastal Eng.*, **55**, 224–235.
- Ardhuin, F. and T. H. C. Herbers, 2002: Bragg scattering of random surface gravity waves by irregular sea bed topography. *J. Fluid Mech.*, **451**, 1–33.
- Ardhuin, F., T. H. C. Herbers, P. F. Jessen and W. C. O’Reilly, 2003a: Swell transformation across the continental shelf. Part II: Validation of a spectral energy balance equation. *J. Phys. Oceanogr.*, **33**, 1940–1953.
- Ardhuin, F., A. D. Jenkins and K. A. Belibassakis, 2008a: Comments on “The three-dimensional current and surface wave equations” by George Mellor. *J. Phys. Oceanogr.*, **38**, 1340–1350.
- Ardhuin, F., W. C. O’Reilly, T. H. C. Herbers and P. F. Jessen, 2003b: Swell transformation across the continental shelf. Part I: Attenuation and directional broadening. *J. Phys. Oceanogr.*, **33**, 1921–1939.
- Ardhuin, F., N. Raschle and K. A. Belibassakis, 2008b: Explicit wave-averaged primitive equations using a generalized Lagrangian mean. *Ocean Mod.*, **20(1)**, 35–60.
- Ardhuin, F., W. E. Rogers, A. V. Babanin, J.-F. Filipot, R. Magne, A. Roland, A. J. van der Westhuysen, P. Queffelec, J.-M. Lefevre, L. Aouf and F. Collard, 2010: Semi-empirical dissipation source functions for ocean waves: Part I, definitions, calibration. *J. Phys. Oceanogr.*, **40(9)**, 1917–1941, doi: 10.1175/2010JPO4324.1.
- Ardhuin, F. and A. Roland, 2012: Coastal wave reflection, directional spread, and seismo-acoustic noise sources. *J. Geophys. Res.*, **117**, doi:10.1029/2011JC007832.
- Babanin, A. V., H.-H. Hwung, I. Shugan, A. Roland, A. J. van der Westhuysen, A. Chawla and C. Gaudier, 2011: Nonlinear waves on collinear currents with horizontal velocity gradient. in *Proc 12th International Workshop on Wave Hindcasting and Forecasting, Kohala Coast, Hawaii*.
- Barber, N. F., 1949: Behaviour of waves on tidal streams. *Proc. Roy. Soc. London*, **A198**, 81–93.
- Battjes, J. A. and S. Beji, 1992: Breaking waves propagating over a shoal. in *Proc. 25th Int. Conf. Coastal Eng.*, pp. 42–50. ASCE.
- Battjes, J. A. and J. P. F. M. Janssen, 1978: Energy loss and set-up due to breaking of random waves. in *Proc. 16th Int. Conf. Coastal Eng.*, pp. 569–587. ASCE.
- Battjes, J. A. and M. J. F. Stive, 1985: Calibration and verification of a dissipation model for random breaking waves. *J. Geophys. Res.*, **90, C5**, 9159–9167.
- Becq-Girard, F., P. Forget and M. Benoit, 1999: Non-linear propagation of unidirectional wave fields over varying topography. *Coastal Eng.*, **38**, 91–113.
- Benney, D. and P. Saffman, 1966: Nonlinear interactions of random waves. *Proc. Roy. Soc. London*, **A289**, 301–321.
- Bennis, A.-C. and F. Ardhuin, 2011: Comments on “the depth-dependent current and wave interaction equations: a revision”. *J. Phys. Oceanogr.*, **41**, 2008–2012.
- Benoit, M., F. Marcos and F. Becq, 1996: Development of a third generation shallow water wave model with unstructured spatial meshing. in *Proc. 25th Int. Conf. Coastal Eng., Orlando, USA*, pp. 465–478. ASCE.

- Berkhoff, J. C. W., 1972: Computation of combined refraction-diffraction. in *Proc. 13th Int. Conf. Coastal Eng., Vancouver, Canada*, pp. 471–490. ASCE.
- Bidlot, J., S. Abdalla and P. Janssen, 2005: A revised formulation for ocean wave dissipation in CY25R1. memo. r60.9/jb/0516. Tech. rep., Res. Dep., ECMWF, Reading, U.K.
- Boers, M., 1996: Simulation of a surf zone with a barred beach; Report 1: Wave heights and wave breaking. Tech. rep., Communications on Hydraulics and Geotechnical Engineering. Fac. of Civil Engineering, Delft University of Technology, Delft, The Netherlands, Available at: <http://repository.tudelft.nl>.
- Booij, N., I. G. Haagsma, L. H. Holthuijsen, A. T. M. M. Kieftenburg, R. C. Ris, A. J. van der Westhuyesen and M. Zijlema, 2004: SWAN Cycle III version 40.41, User Manual. Tech. rep., Delft University of Technology, Delft, The Netherlands.
- Booij, N., R. C. Ris and L. H. Holthuijsen, 1999: A third-generation wave model for coastal regions, Part I, Model description and validation. *J. Geophys. Res.*, **104**, 7649–7666.
- Bouws, E. and G. J. Komen, 1983: On the balance between growth and dissipation in an extreme depth-limited wind-sea in the southern North Sea. *J. Phys. Oceanogr.*, **13**, 1653–1658.
- Chawla, A. and J. T. Kirby, 2002: Monochromatic and random wave breaking at blocking points. *J. Geophys. Res.*, **107(C7)**, 10.1029/2001JC001042.
- Chen, Y. R., R. T. Guza and S. Elgar, 1997: Modeling spectra of breaking surface waves in shallow water. *J. Geophys. Res.*, **102**, 20035–25046.
- Collins, J. I., 1972: Prediction of shallow water spectra. *J. Geophys. Res.*, **77(15)**, 2693–2707.
- Cook, J., M. Frost, G. Love, L. Phegley, Q. Zhao, D. A. Geiszler, J. Kent, S. Potts, D. Martinez, T. J. N. abd D. Dismachek and L. N. McDerimid, 2007: The U.S. Navy’s on-demand, coupled, mesoscale data assimilation and prediction system. in *22nd Conference on Weather Analysis and Forecasting/18th Conference on Numerical Weather Prediction, Paper P2.1*. AMS.
- Dalrymple, R. A., J. T. Kirby and P. A. Hwang, 1984: Wave diffraction due to areas of energy dissipation. *J. of Waterway, Port, Coastal and Ocean Eng.*, **110**, 67–79.
- Dalrymple, R. A. and P. L. Liu, 1978: Waves over soft mud beds: A two-layer fluid mud model. *J. Phys. Oceanogr.*, **8**, 1121–1131.
- De Wit, P. J. D., 1995: *Liquefaction of cohesive sediment by waves*. Ph.D. thesis, Delft Univ. of Technology, Delft, The Netherlands.
- Dietrich, J. C., M. Zijlema, J. J. Westerink, L. H. Holthuijsen, C. Dawson, R. A. Luetlich, Jr., R. Jensen, J. M. Smith, G. S. Stelling and G. W. Stone, 2011: Modeling hurricane waves and storm surge using integrally-coupled, scalable computations. *Coastal Eng.*, **58**, 45–65.
- Doering, J. C. and A. J. Bowen, 1995: Parametrization of orbital velocity asymmetries of shoaling and breaking waves using bispectral analysis. *Coastal Eng.*, **26**, 1-2, 15–33.
- Duncan, 1981: An experimental investigation of breaking waves produced by a towed hydrofoil. *Proc. Roy. Soc. Lond. A*, **377**, 331–348.
- Duncan, 1983: The breaking and non-breaking wave resistance of a two-dimensional hydrofoil. *J. Fluid Mech.*, **126**, 507–520.
- Eldeberky, Y., 1996: *Nonlinear transformations of wave spectra in the nearshore zone*. Ph.D. thesis, Delft Univ. of Technology, Delft, The Netherlands, 203 pp.

- Eldeberky, Y. and P. A. Madsen, 1999: Deterministic and stochastic evolution equations for fully dispersive and weakly non-linear waves. *Coastal Eng.*, **38**, 1–24.
- Filipot, J.-F. and F. Ardhuin, 2012: A unified spectral parameterization for wave breaking: From the deep ocean to the surf zone. *J. Geophys. Res.*, **117**, C00J08, doi:10.1029/2011JC007784.
- Filipot, J.-F., F. Ardhuin and A. V. Babanin, 2010: A unified deep-to-shallow water wave breaking probability parameterization. *J. Geophys. Res.*, **115**, C04022, doi:10.1029/2009JC005448.
- Gade, H. G., 1958: Effects of a non-rigid, impermeable bottom on plane surface waves in shallow water. *J. Mar. Res.*, **16**(2), 61–82.
- Graber, H. C. and O. S. Madsen, 1988: A finite-depth wind-wave model. Part I: Model description. *J. Phys. Oceanogr.*, **18**, 1465–1483.
- Grant, W. D. and O. S. Madsen, 1982: Movable bed roughness in unsteady oscillatory flow. *J. Geophys. Res.*, **87** (C1), 469–481.
- Hasselmann, K., 1962: On the non-linear transfer in a gravity wave spectrum, Part 1. General theory. *J. Fluid Mech.*, **12**, 481–500.
- Hasselmann, K., 1966: Feynman diagrams and interaction rules of wave-wave scattering processes. *Rev. Geophys.*, **4**, 1–32.
- Hasselmann, K., T. P. Barnett, E. Bouws and H. C. et al., 1973: Measurement of wind-wave growth and swell decay during the joint north sea wave project (jonswap). *Dtsch. Hydrogr. Z. Suppl.*, **A(8)**, **12**, 95 pp.
- Hasselmann, K. and J. I. Collins, 1968: Spectral dissipation of finite depth gravity waves due to turbulent bottom friction. *J. Mar. Res.*, **26**, 1–12.
- Haus, B. K., 2007: Surface current effects on the fetch-limited growth of wave energy. *J. Geophys. Res.*, **112**, C03003, doi:10.1029/2006JC003924.
- Herbers, T. H. C. and M. C. Burton, 1997: Nonlinear shoaling of directionally spread waves on a beach. *J. Geophys. Res.*, **102**, 21101–21114.
- Herbers, T. H. C., M. Orzech, S. Elgar and R. T. Guza, 2003: Shoaling transformation of wave frequency-directional spectra. *J. Geophys. Res.*, **108**, doi:10.1029/2001JC001304.
- Herbers, T. H. C., N. R. Rossnogle and S. Elgar, 2000: Spectral energy balance of breaking waves within the surf zone. *J. Phys. Oceanogr.*, **30**, 2723–2737.
- Hersbach, H. and J.-R. Bidlot, 2008: The relevance of ocean surface current in the ECMWF analysis and forecast system. in *Proceeding from the ECMWF Workshop on Atmosphere-Ocean Interaction, 10-12 November 2008*. ECMWF, Reading, U.K.
- Holloway, G., 1980: Oceanic internal waves are not weak waves. *J. Phys. Oceanogr.*, **10**, 906–914.
- Holthuijsen, L. H., A. Herman and N. Booij, 2003: Phase-decoupled refraction-diffraction for spectral wave models. *Coastal Eng.*, **49**, 291–305.
- Holthuijsen, L. H. and H. L. Tolman, 1991: Effects of the Gulf Stream on ocean waves. *J. Phys. Oceanogr.*, **96**(C7), 12755–12771.
- Hsu, T.-W., J. M. Liao and S. H. Ou, 2006: WWM extended to account for wave diffraction on a current over a rapidly varying topography. in *In 3rd Chinese-German Joint Symp. Coastal and Ocean Engineering, 8–16 November 2006*. Taiwan: Coastal Ocean Monitoring Center, National Cheng Kung University.

- Hsu, T.-W., S.-H. Ou and J.-M. Liau, 2005: Hindcasting nearshore wind waves using a FEM code for SWAN. *Coastal Eng.*, **52**, 2, 177–195.
- Ilic, S., A. J. van der Westhuysen, J. Roelvink and A. Chadwick, 2007: Multi-directional wave transformation around detached breakwaters. *Coastal Eng.*, **54**, 775–789.
- IPET, 2009: Performance evaluation of the New Orleans and Southeast Louisiana Hurricane Protection System. Tech. Rep. Final report of the Interagency Performance Evaluation Task Force, Volume I Executive Summary and Overview, U.S. Army Corps of Engineers.
- Janssen, T. T., 2006: *Nonlinear surface waves over topography*. Ph.D. thesis, Delft Univ. of Technology, Delft, The Netherlands, 208 pp.
- Janssen, T. T., T. H. C. Herbers and J. A. Battjes, 2008: Evolution of ocean wave statistics in shallow water: refraction and diffraction over seafloor topography. *J. Geophys. Res.*, **113**, C03024.
- Jonsson, I. G., 1966: Wave boundary layers and bottom friction. in *Proc. 10th Int. Conf. Coastal Eng., Tokyo, Japan*, pp. 127–148. ASCE.
- Jonsson, I. G., 1980: A new approach to oscillatory rough turbulent boundary layers. *Ocean Eng.*, **7**, 109–152.
- Jonsson, I. G. and N. A. Carlsen, 1976: Experimental and theoretical investigations in an oscillatory turbulent boundary layer. *J. Hydraul. Res.*, **14**, 45–60.
- Kobayashi, N., A. W. Raichle and T. Asano, 1993: Wave attenuation by vegetation. *J. of Waterway, Port, Coastal and Ocean Eng.*, **119**, 30–48.
- Kofoed-Hanssen, H. and J. H. Rasmussen, 1998: Modelling of nonlinear shoaling based on stochastic evolution equations. *Coastal Eng.*, **33**, 203–232.
- Kranenburg, W. M., J. C. Winterwerp, G. J. de Boer, J. M. Cornelisse and M. Zijlema, 2011: SWAN-Mud: Engineering model for mud-induced wave damping. *J. Hydr. Eng.*, **Vol. 137, No. 9**, 959–975.
- Lai, R. J., S. R. Long and N. E. Huang, 1989: Laboratory studies of wave-current interaction: Kinematics of the strong interaction. *J. Geophys. Res.*, **94**, 16201–16214.
- Liu, P. L.-F., 1973: Damping of water waves over porous bed. *J. Hydraul. Div.*, **99(12)**, 2263–2271.
- Long, R. B., 1973: Scattering of surface waves by an irregular bottom. *J. Geophys. Res.*, **78(33)**, 7861–7870.
- Maa, P.-Y., 1986: *Erosion of soft mud beds by waves*. Ph.D. thesis, Coastal and Oceanographic Engineering Dept., Univ. of Florida, Gainesville, FL.
- MacPherson, H., 1980: The attenuation of water wave over a non-rigid bed. *J. Fluid Mech.*, **97(4)**, 721–742.
- Madsen, O. S., Y.-K. Poon and H. C. Graber, 1988: Spectral wave attenuation by bottom friction. in *Proc. 21st Int. Conf. Coastal Eng., Malaga, Spain*, pp. 492–504. ASCE.
- Mehra, A. and I. Rivin, 2010: A real time ocean forecast system for the north atlantic ocean. *Terr. Atmos. Ocean. Sci.*, **Vol. 21, No. 1**, 211–228, doi: 10.3319/TAO.2009.04.16.01(IWNOP).
- Mei, C. C., 1983: *The applied dynamics of ocean surface waves*. Wiley, New York, 740 pp.
- Mei, C. C. and K. F. Liu, 1987: A Bingham plastic model for a muddy seabed under long waves. *J. Geophys. Res.*, **92(C13)**, 14581–14594.

- Mellor, G., 2003: The three-dimensional current and surface wave equations. *J. Phys. Oceanogr.*, **33**, 1978–1989.
- Mellor, G., 2005: Some consequences of the three-dimensional current and surface wave equations. *J. Phys. Oceanogr.*, **35**, 2291–2298.
- Mellor, G., 2011a: Corrigendum. *J. Phys. Oceanogr.*, **41(7)**, 1417–1418.
- Mellor, G., 2011b: Wave radiation stress. *Ocean Dynamics*, **61**, 563–568.
- Mendez, F. M. and I. J. Losada, 2004: An empirical model to estimate the propagation of random breaking and nonbreaking waves over vegetation fields. *Coastal Eng.*, **51**, 103–118.
- Miche, A., 1944: Mouvements ondulatoires de la mer en profondeur croissante ou décroissante. Forme limite de la houle lors de son déferlement. Application aux digues maritimes. Troisième partie. Forme et propriétés des houles limites lors du déferlement. Croissance des vitesses vers la rive. *Ann. Ponts Chaussees*, **114**, 369–406.
- Mirfenderesk, H., 1999: *The dissipation of ocean wave spectra due to bottom friction*. Ph.D. thesis, University of New South Wales, Australian Defence Force Academy, Canberra, Australia.
- Mirfenderesk, H. and I. R. Young, 2003: Direct measurements of the bottom friction factor beneath surface gravity waves. *Applied Ocean Research*, **25(5)**, 269–287.
- Morrison, J. R. M., M. P. O'Brien, J. W. Johnson and S. A. Schaaf, 1950: The force exerted by surface waves on piles. *Petrol. Trans.*, **AWME 189**.
- Nelson, R. C., 1994: Depth limited design wave heights in very flat regions. *Coastal Eng.*, **23**, 43–59.
- Ng, C.-O., 2000: Water waves over a muddy bed: A two layer Stokes' boundary layer model. *Coastal Eng.*, **40**, 221–242.
- Nielsen, P., 1992: Coastal bottom boundary layer and sediment transport. in *Advanced Series on Ocean Engineering*, p. 324 pp. World Scientific.
- Phillips, O. M., 1977: *The dynamics of the upper ocean, Second Edition*. Cambridge Univ. Press, 336 pp.
- Quartel, S., A. Kroon, P. Augustinus, P. V. Santen and N. H. Tri, 2007: Wave attenuation in coastal mangroves in the Red River Delta, Vietnam. *J. Asian Earth Sci.*, **29(4)**, 115–141.
- Ris, R. C. and L. H. Holthuijsen, 1996: Spectral modelling of current wave-blocking. in *Proc. 25th Int. Conf. Coastal Eng., Orlando, USA*, pp. 1247–1254. ASCE.
- Rogers, W. E. and K. T. Holland, 2009: A study of dissipation of wind-waves by mud at cassino beach, brazil: Prediction and inversion. *Coastal Shelf Res.*, **29(3)**, 676–690.
- Roland, A., 2008: *Development of WWM II: Spectral wave modelling on unstructured meshes*. Ph.D. thesis, Inst. of Hydraul. and Water Resour. Eng., Techn. Univer. Darmstadt, Darmstadt, Germany.
- Ruessink, B. G., D. J. R. Walstra and H. N. Southgate, 2003: Calibration and verification of a parametric wave model on barred beaches. *Coastal Eng.*, **48**, 139–149.
- Salmon, J. and L. H. Holthuijsen, 2011: Re-scaling the Battjes-Janssen model for depth-induced wave-breaking. in *Proc. 12th Int. Workshop on Wave Hindcasting and Forecasting, Hawaii*. JCOMM.

- Settelmaier, J. B., A. Gibbs, P. Santos, T. Freeman and D. Gaer, 2011: Simulating Waves Nearshore (SWAN) modeling efforts at the National Weather Service (NWS) Southern Region (SR) coastal Weather Forecast Offices (WFOs). in *Proc. 91th AMS Annual Meeting, Seattle, WA, Paper P13A.4*. AMS.
- Shemdin, O., K. Hasselmann, S. V. Hsiao and K. Heterich, 1978: Nonlinear and linear bottom interaction effects in shallow water. in *Turbulent Fluxes through the Sea Surface, Wave Dynamics and Prediction*, pp. 347–365. NATO Conf. Ser. V, Vol. 1.
- Shyu, J. H. and O. Phillips, 1990: The blockage of gravity and capillary waves by longer waves and currents. *J. Fluid Mech.*, **217**, 115–141.
- Smith, G., A. V. Babanin, P. Riedel, I. R. Young, S. Oliver and G. Hubbert, 2011: Introduction of a new friction routine in the SWAN model that evaluates roughness due to bedform and sediment size changes. *Coastal Eng.*, **58**, **4**, 317–326.
- Soltanpour, M., T. Shibayama and T. Noma, 2003: Cross-shore mud transport and beach deformation model. *Coastal Eng. J.*, **45**(3), 363–386.
- Stiassnie, M. and N. Drimer, 2006: Prediction of long forcing waves for harbor agitation studies. *J. Waterway, Port, Coastal, Ocean Eng.*, **132**, 166–171.
- Stoker, J., 1957: *Water Waves: The Mathematical Theory With Applications*. Interscience, New York.
- Suastika, I. K., 2004: *Wave blocking*. Ph.D. thesis, Delft Univ. of Technology, Delft, The Netherlands, 157 pp.
- Suzuki, T., M. Zijlema, B. Burger, M. C. Meijer and S. Narayan, 2011: Wave dissipation by vegetation with layer schematization in SWAN. *Coastal Eng.*, **59**, 64–71.
- The WISE Group, 2007: Wave modelling: The state of the art. *Progress in Oceanography*, **75**, **4**, 603–674.
- Thornton, E. B. and R. T. Guza, 1983: Transformation of wave height distribution. *J. Geophys. Res.*, **88**, 5925–5938.
- Toledo, Y. and Y. Agnon, 2012: Stochastic evolution equations with localized nonlinear shoaling coefficients. *European Journal of Mechanics - B/Fluids*, **34**, 13–18.
- Toledo, Y., T.-W. Hsu and A. Roland, 2012: Extended time-dependent mild-slope and wave-action equations for wave-bottom and wave-current interactions. *Proc. Roy. Soc. Lond. A*, **468**, 184–205, doi:10.1098/rspa.2011.037.
- Tolman, H. L., 1991: A third-generation model for wind waves on slowly varying, unsteady and inhomogeneous depths and currents. *J. Phys. Oceanogr.*, **21**, 782–797.
- Tolman, H. L., 1994: Wind waves and moveable-bed bottom friction. *J. Phys. Oceanogr.*, **24**, 994–1009.
- Tolman, H. L., 1995: Subgrid modeling of moveable-bed bottom friction in wind wave models. *Coastal Eng.*, **26**, 57–75.
- Tolman, H. L., 2008: A mosaic approach to wind wave modeling. *Ocean Mod.*, **25**, 35–47.
- Tolman, H. L., B. Balasubramanian, L. D. Burroughs, D. V. Chalikov, Y. Y. Chao, H. S. Chen and V. M. Gerald, 2002: Development and implementation of wind generated ocean surface wave models at NCEP. *Weather and Forecasting*, **17**, 311–333.

- Van der Westhuysen, A. J., 2009: Modelling of depth-induced wave breaking over sloping and horizontal beds. in *Proc. 11th Int. Workshop on Wave Hindcasting and Forecasting*. JCOMM.
- Van der Westhuysen, A. J., 2010: Modelling of depth-induced wave breaking under finite-depth wave growth conditions. *J. Geophys. Res.*, **115**, C01008, doi:10.1029/2009JC005433.
- Van der Westhuysen, A. J., 2012: Spectral modeling of wave dissipation on negative current gradients. *Coastal Eng.*, **68**, 17–30.
- Van der Westhuysen, A. J., R. Padilla, T. Nicolini, S. Tjaden, J. Settelmaier, A. Gibbs, P. Santos, J. Maloney, T. Freeman, D. Gaer, M. Willis, N. Kurkowski and J. Kuhn, 2011: Development of the Nearshore Wave Prediction System (NWPS) (poster). *12th Int. Workshop on Wave Hindcasting and Forecasting and 3rd Coastal Hazards Symposium (WAVES 2011)*.
- Van der Westhuysen, A. J. and T. L. Tolman, 2011: Quasi-stationary WAVEWATCH III for the nearshore. in *Proc. 12th Int. Workshop on Wave Hindcasting and Forecasting, Hawaii*. JCOMM.
- Van der Westhuysen, A. J., A. van Dongeren, J. Groeneweg, G. van Vledder, H. Peters, C. Gautier and J. C. C. van Nieuwkoop, 2012: Improvements in spectral wave modeling in tidal inlet seas. *J. Geophys. Res.*, **117**, doi:10.1029/2011JC007837.
- Van der Westhuysen, A. J., M. Zijlema and J. A. Battjes, 2007: Nonlinear saturation-based whitecapping dissipation in SWAN for deep and shallow water. *Coastal Eng.*, **54**, 151–170.
- Verbeek, H. and J. M. Cornelisse, 1997: *Erosion and liquefaction of natural mud under surface waves*. Cohesive sediments, N. Burt, R. Parker, and J. Watts, eds., Wiley, New York, 353–364.
- Vo-Luong, P. and S. Massel, 2008: Energy dissipation in non-uniform mangrove forests of arbitrary depth. *J. Mar. Sys.*, **74**, 603–622.
- WAMDIG, 1988: The WAM model—a third generation ocean wave prediction model. *J. Phys. Oceanogr.*, **18**, 1775–1809.
- Willebrand, J., 1975: Energy transport in a nonlinear and inhomogeneous random gravity wave field. *J. Fluid Mech.*, **70**, 113–126.
- Young, I. R. and A. V. Babanin, 2006: The form of the asymptotic depth-limited wind wave frequency spectrum. *J. Geophys. Res.*, **111**, C06031, doi:10.1029/2005JC003398.
- Zhang, F. W., W. M. Drennan, B. K. Haus and H. C. Graber, 2009: On wind-wave-current interactions during the Shoaling Waves Experiment. *J. Geophys. Res.*, **114**, C01018, doi:10.1029/2008JC004998.
- Zijlema, M., 2010: Computation of wind-wave spectra in coastal waters with SWAN on unstructured grids. *Coastal Eng.*, **57**, 3, 267–277.
- Zijlema, M., G. P. van Vledder and L. H. Holthuijsen, 2012: Bottom friction and wind drag for wave models. *Coastal Eng.*, **65**, 19–26.